


## RESEARCH ARTICLE

# Anticandidal activity of synthetic peptides: Mechanism of action revealed by scanning electron and fluorescence microscopies and synergism effect with nystatin

Patrícia G. Lima<sup>1</sup> | Pedro F.N. Souza<sup>1</sup>  | Cleverson D.T. Freitas<sup>1</sup> |  
Jose T.A. Oliveira<sup>1</sup> | Lucas P. Dias<sup>1</sup> | João X.S. Neto<sup>1</sup> | Ilka M. Vasconcelos<sup>1</sup> |  
José L.S. Lopes<sup>2</sup> | Daniele O.B. Sousa<sup>1</sup>

<sup>1</sup>Department of Biochemistry and Molecular Biology, Federal University of Ceará, Fortaleza, Brazil

<sup>2</sup>Department of Applied Physics, University of Sao Paulo, Sao Paulo, Brazil

## Correspondence

Pedro F. N. Souza and Daniele O. B. Sousa, Laboratory of Plant Defense Proteins, Department of Biochemistry and Molecular Biology, Federal University of Ceará, Ave Mister Hull, PO Box 60451 Fortaleza, CE, Brazil.  
Email: pedrofilhobio@gmail.com; daniele.sousa@ufc.br

## Funding information

Conselho Nacional de Desenvolvimento Científico e Tecnológico; Coordenação de Aperfeiçoamento de Pessoal de Nível Superior – National Institute of Science and Technology of Bioinspiration, Grant/Award Number: 465507/2014-0; São Paulo State Research Foundation, Grant/Award Number: 2018/19546-7; National Council for Scientific and Technological Development, Grant/Award Numbers: 306202/2017-4, 308107/2013-6

*Candida albicans* has emerged as a major public health problem in recent decades. The most important contributing factor is the rapid increase in resistance to conventional drugs worldwide. Synthetic antimicrobial peptides (SAMPs) have attracted substantial attention as alternatives and/or adjuvants in therapeutic treatments due to their strong activity at low concentrations without apparent toxicity. Here, two SAMPs, named Mo-CBP<sub>3</sub>-PepI (CPAIQRCC) and Mo-CBP<sub>3</sub>-PepII (NIQPPCRCC), are described, bioinspired by Mo-CBP<sub>3</sub>, which is an antifungal chitin-binding protein from *Moringa oleifera* seeds. Furthermore, the mechanism of anticandidal activity was evaluated as well as their synergistic effects with nystatin. Both peptides induced the production of reactive oxygen species (ROS), cell wall degradation, and large pores in the *C. albicans* cell membrane. In addition, the peptides exhibited high potential as adjuvants because of their synergistic effects, by increasing almost 50-fold the anticandidal activity of the conventional antifungal drug nystatin. These peptides have excellent potential as new drugs and/or adjuvants to conventional drugs for treatment of clinical infections caused by *C. albicans*.

## KEYWORDS

anticandidal action, *Candida albicans*, cell wall rupture, Mo-CBP<sub>3</sub> peptides, pore formation, synthetic antimicrobial peptide

## 1 | INTRODUCTION

The increase of antimicrobial resistance to conventional drugs is expanding globally, posing a serious threat to the current strategies employed to treat infectious diseases. This is caused by two major problems: (1) the misuse and overuse of antimicrobial drugs and (2) uncontrolled prescription, where up to 50% of drugs prescribed are unnecessary.<sup>1–4</sup>

Infections caused by fungi have been increasing rapidly worldwide. Currently, over 300 million people are infected with some type of fungi every year, leading to 1,350,000 deaths annually.<sup>5</sup> The major fungi responsible for human diseases belong to the *Candida* genus,<sup>6</sup> and transplant and cancer patients and those submitted to any type of immune-suppressive therapy are most commonly affected.<sup>5–7</sup>

The global prevalence of fungal infections caused by *Candida* species is estimated to be 7 cases per 100 patients. In the United States and Europe, *Candida* species are responsible for hospital-acquired bloodstream infections, leading to high mortality, prolonged hospital stays, and elevated healthcare costs.<sup>5–9</sup> The epidemiology of *Candida* infections has changed over the years. In 2010, *Candida albicans*

Patrícia G. Lima, Pedro F. N. Souza, Cleverson D. T. Freitas, and Daniele O.B. Sousa contribute equally to this work.

broadly resistant to many conventional antifungals available was responsible for up to 70% of the clinical infections.<sup>7</sup> However, a new study in 2017 showed alterations in this scenario. The incidence of infection caused by non-*C. albicans* today reaches 56.5% of candidemia cases. This value is divided among several non-*C. albicans* species, such as *C. glabrata* (33.3%), *C. tropicalis* (20.3%), *C. parapsilosis* (1.4%), and *C. kefyr* (1.4%). *C. albicans* is still the leading cause and most responsible for candidemia, in 43.5% of the patients.<sup>10</sup>

To face this global health challenge, synthetic antimicrobial peptides (SAMPs) have emerged as new drugs or even as adjuvants to commercial drugs<sup>11,12</sup> because the development of new technologies has allowed the reduction of costs for synthesis and achieving high purity, as well as making it possible to obtain SAMPs with specific modifications, such as cyclization, alanine scanning, or amino acid substitution.<sup>11–13</sup> Generally, SAMPs are positively charged and have amphipathic properties, enabling them to interact with cell membranes, inducing pore formation.<sup>13</sup>

Recently, our research group characterized and evaluated the antimicrobial activity of many SAMPs against bacteria and yeasts pathogenic to humans.<sup>13–15</sup> For example, Dias et al.<sup>14</sup> reported that R<sub>c</sub>Alb-PeplI (SLRGCC) is a small (637.77 Da), positively charged (+1), and slightly (pI 7.80) basic peptide with hydrophobicity of 50%, derived from an antimicrobial 2S albumin purified from *Ricinus communis* seed cake,<sup>16</sup> and a potent antimicrobial peptide against *C. parapsilosis* and *Klebsiella pneumoniae*. Lopes et al.<sup>15</sup> reported that a synthetic peptide derived from a thaumatin protein induces apoptosis in *C. albicans*. Mo-CBP<sub>3</sub>-Pepl (893.12 Da) and Mo-CBP<sub>3</sub>-PeplI (1033.26 Da) are both small, slightly basic, and positively charged, with hydrophobicity of 62 and 44%, respectively, derived from Mo-CBP<sub>3</sub>, with IC<sub>90</sub> values against *C. albicans* of 2.2 and 17.5  $\mu$ M, respectively.<sup>13</sup> Bioinformatic analyses revealed the potential of these peptides to penetrate cells without toxicity to human cells. Despite the strong activity of those peptides, their mechanisms of action and toxicity are still unknown. Therefore, this new study was focused on providing information about the mechanism behind the anticandidal activity of Mo-CBP<sub>3</sub>-Pepl and Mo-CBP<sub>3</sub>-PeplI and their toxicity to mammalian cells, as well as evaluating their synergic effects with nystatin (NYS), a leading conventional drug used to treat infections caused by *Candida* species.

## 2 | MATERIALS AND METHODS

### 2.1 | Peptide design and characterization

Mo-CBP<sub>3</sub>-Pepl (CPAIQRCC) and Mo-CBP<sub>3</sub>-PeplI (NIQPPCRCC) were designed employing the same criteria described by Oliveira et al.,<sup>13</sup> which were low molecular size (600–1200 Da), at least 40% hydrophobic potential, positive net charge (at least +1), and a Boman index  $\leq 2.5$ . The peptides were purchased from the company GenOne (São Paulo, Brazil). The quality and purity ( $\geq 95\%$ ) were determined by reverse-phase high-performance liquid chromatography (RP-HPLC) and mass spectrometry (MS), according to Lopes et al.<sup>15</sup>

### 2.2 | Circular dichroism and synchrotron radiation circular dichroism spectroscopies

Synchrotron radiation circular dichroism (SRCD) spectroscopy was employed to investigate the conformation of the peptides either in aqueous solution or in partially dehydrated films. Measurements of Mo-CBP<sub>3</sub>-Pepl (1.6 mg/ml) and Mo-CBP<sub>3</sub>-PeplI (2.2 mg/ml) in 10 mM sodium phosphate buffer (pH 7.4) or in 50% trifluoroethanol (TFE) were performed over the wavelength range from 170 to 270 nm, with a bandwidth of 1 nm and allowing 2-s dwell time, using in a Suprasil quartz cuvette with 0.0098-cm pathlength (Hellma Ltd, UK), at 25°C. The SRCD spectra of the peptides (0.7 nmol) in the dehydrated film deposited on the surface of a quartz-glass plate were collected over the wavelength range from 155 to 280 nm, with a bandwidth of 1 nm, at 25°C, taking four successive rotations of the plate at 0, 90, 180, and 270° in order to avoid any linear dichroism effect. All the SRCD experiments were carried out at the synchrotron facility Aarhus STorage Ring in Denmark 2 (ASTRID2) in the AU-CD beamline (Aarhus Circular Dichroism, Aarhus, Denmark). The possible interaction of both peptides (0.3 mg/ml) with artificial micelles was evaluated by measurements of conventional circular dichroism (CD) spectroscopy with a Jasco J-715 spectropolarimeter, as the average of six scans over the wavelength from 190 to 270 nm, with a bandwidth of 1 nm, using a 0.1-cm pathlength quartz cuvette, at 25°C. Peptides (0.3 mg/ml) were incubated with micelles made of 20 mM of sodium dodecyl sulfate (SDS) or 20 mM of *N*-hexadecyl-*N*-*N'*-dimethyl-3-ammonia-1-propane-sulfonate (HPS) according to previous studies.<sup>14,17,18</sup> HPS was chosen because it has been used to completely mimic zwitterionic micelles, especially for taking CD measurements, because of the low background absorption of the micellar system in the far-UV region.<sup>14</sup> All the CD/SRCD spectra were processed using the CDToolX software.<sup>19</sup>

### 2.3 | Anticandidal assay

The anticandidal assays against *C. albicans* (American Type Culture Collection [ATCC] 10231) were performed as described by Neto et al.,<sup>20</sup> who made some modifications from the method described by the Clinical & Laboratory Standards Institute (CLSI).<sup>21</sup> The media used in this assay was potato dextrose broth (PDB). *C. albicans* cells ( $2.5 \times 10^3$  CFU/ml) were prepared in PDB media from an culture grown overnight in potato dextrose agar (PDA) at 35°C. One hundred microliters of *C. albicans* suspension ( $2.5 \times 10^3$  CFU/ml) was incubated with 100  $\mu$ l of Mo-CBP<sub>3</sub>-Pepl and Mo-CBP<sub>3</sub>-PeplI at 2.2 and 17.5  $\mu$ M, respectively, to reach the IC<sub>90</sub> in flat bottom 96-well plates at 37°C for 24 h, and absorbance was read using an automated microplate reader (Epoch, BioTek). The concentration of peptides that inhibited *C. albicans* growth by 90%, as defined by Oliveira et al.,<sup>13</sup> was employed. The positive control for cell integrity was a solution composed of 0.15 M NaCl in 5% dimethyl sulfoxide (DMSO) (DMSO-NaCl). Nystatin was used negative control of cell integrity. The assay was repeated three times.

## 2.4 | Detection of ROS overproduction and cell membrane integrity assay

To evaluate the peptide-induced ROS generation, the method described by Maurya et al.<sup>22</sup> was employed, using 2',7'-dichlorofluorescein diacetate (DCFH-DA). *C. albicans* cells were cultured in PDB media for 18 h at 37°C. Then, the cell concentration was standardized to  $2.5 \times 10^3$  CFU/ml, and then, 100  $\mu$ l of cells was incubated with 100  $\mu$ l of *Mo*-CBP<sub>3</sub>-Pepl (2.2  $\mu$ M) or *Mo*-CBP<sub>3</sub>-Pepll (17.5  $\mu$ M) at 37°C for 24 h, without light. Nystatin and the solution composed of 0.15 M NaCl in 5% DMSO (DMSO-NaCl) were used as negative and positive controls, respectively. After incubation, cells were washed three times with 0.15 M NaCl to remove PDB media and then were mixed with 10  $\mu$ M of DCFH-DA for 30 min at 37°C. After the incubation time, the cells were centrifuged (Mikro 200R centrifuge, Germany) at 3,000 g for 5 min at 22°C and washed again as mentioned. Finally, sample cells were mounted on a glass plate for observation under a fluorescence microscope (Olympus System BX60) with excitation wavelength of 488 nm and emission wavelength of 525 nm.

To assess the pore formation induced by peptides, the method described by Oliveira et al.<sup>12</sup> was employed, using propidium iodide (PI) uptake. The *C. albicans* cells were grown and treated as mentioned above. The samples were washed and incubated with PI at 1  $\mu$ M for 30 min at 37°C. Next, the cells were washed and analyzed under a fluorescence microscope (Olympus System BX60) with excitation wavelength of 488 nm and emission wavelength of 525 nm.

In addition, to assess the size of the pores generated, *C. albicans* cells treated with both peptides were also incubated with 10  $\mu$ M of conjugated fluorescein isothiocyanate (FITC)-dextrans with sizes of 6, 10, and 20 kDa (Sigma-Aldrich) to evaluate the diameter of the pores formed. After incubation for 1 h at 37°C in the dark, cells were observed under a fluorescence microscope (Olympus System BX60) with excitation wavelength of 488 nm and emission wavelength of 525 nm, as described by Oliveira et al.<sup>13</sup>

## 2.5 | Scanning electron microscopy analyses

To perform scanning electron microscopy (SEM) analyses, samples were prepared following the method described by Oliveira et al.<sup>13</sup> Briefly, *C. albicans* cells were treated and washed as mentioned. Then the cells were fixed in 1% (v/v) glutaraldehyde +4% (v/v) formaldehyde in 0.15 M of sodium phosphate buffer at pH 7.0. Next the cells were harvested by centrifugation (Mikro 200R centrifuge, Germany—at 3,000 g for 5 min at 22°C), treated with 0.2% (m/v) osmium tetroxide for 30 min, and centrifuged again. Before mounting under a coverslip, the samples were successively dehydrated in ethanol (30%, 70%, 100%, 100%, and 100% [v/v]) for 10 min each, followed by centrifugation. The final dehydration was done with 50/50 ethanol/hexamethyldisilazane (HMDS) for 10 min and then 100% (v/v) HMDS. The material was mounted under coverslips previously treated with 0.1% of gelatin. The coverslips were assembled on stubs

and coated with a 20-nm gold layer using a positron-emission tomography (PET) coating machine (Emitech-Q150TES, Quorum Technologies, England). Images were captured with an FEI Inspect™ 50 scanning electron microscope (Oregon, USA), equipped with a low energy detector (Everhart-Thornley) using acceleration beam voltage of 20,000 kV and 20,000 $\times$  detector magnification.

## 2.6 | Chitin-binding assays

Because *Mo*-CBP<sub>3</sub> is a chitin-binding protein,<sup>23</sup> *Mo*-CBP<sub>3</sub>-Pepl and *Mo*-CBP<sub>3</sub>-Pepll were submitted to affinity chromatography in a chitin column as described before.<sup>13</sup> *Mo*-CBP<sub>3</sub>-Pepl and *Mo*-CBP<sub>3</sub>-Pepll (0.5 mg/ml) were loaded in a previously equilibrated chitin column with a DMSO-NaCl solution. The nonretained peak was eluted with DMSO-NaCl solution, and the retained peaks were eluted sequentially with 0.1 M of acetic acid, 0.1 of M HCl, and 0.1 M of NaOH. The peptides were monitored at 230 nm using an automated absorbance reader (Epoch, BioTek Instruments, Inc., USA).

## 2.7 | Synergism assay

The synergistic effect between NYS and the peptides against *C. albicans* planktonic cells was analyzed according to Lu et al.<sup>24</sup> The *C. albicans* cells were prepared and the assay performed as described before. The concentrations for NYS varied from 108 to 0.03  $\mu$ M, for *Mo*-CBP<sub>3</sub>-Pepl from 2.2 to 0.27  $\mu$ M and for *Mo*-CBP<sub>3</sub>-Pepll from 17.5 to 2.18  $\mu$ M. The anticandidal activity was tested as described by Neto et al.<sup>20</sup> All concentrations for NYS and peptides were tested alone or mixed, forming the groups NYS, *Mo*-CBP<sub>3</sub>-Pepl, *Mo*-CBP<sub>3</sub>-Pepll, NYS + *Mo*-CBP<sub>3</sub>-Pepl, and NYS + *Mo*-CBP<sub>3</sub>-Pepll. Data were analyzed to calculate the fractional inhibitory concentration index (FICI):  $FICI = FIC_N + FIC_P = (IC_N^{comb}/IC_N^{alone}) + (IC_P^{comb}/IC_P^{alone})$ , where  $IC_N^{comb}$  is the inhibitory concentration of NYS combined with *Mo*-CBP<sub>3</sub>-Pepl or *Mo*-CBP<sub>3</sub>-Pepll, and  $IC_N^{alone}$  is the same definition applied to  $IC_P^{comb}$  and  $IC_P^{alone}$ . The FICI values indicate antagonistic (FICI  $\geq 4.0$ ), indifferent (FICI 0.5–4.0), or synergistic (FICI  $\leq 0.5$ ) effect.<sup>24</sup>

## 2.8 | Hemolytic assay

The hemolytic assay of peptides against type A, B, and O human red blood cells (HRBCs) was performed following the method described by Oliveira et al.<sup>13,14</sup> The three types of HRBCs were chosen to obtain more information about the possible toxicity of the peptides. For clinical applications, peptides cannot present any kind of toxicity to these cells. The HRBCs from A, B, and O were kindly provided by the Ceará Hematology and Hemotherapy Center (Brazil). The blood was collected in the presence of heparin (5 IU/ml) from unknown and healthy donors. The HRBCs were recovered by centrifugation at 300 g for 5 min at 4°C (Mikro 200R centrifuge, Hettich, Germany) and

resuspended in 0.15 M NaCl. After washing three times with 0.15 M NaCl, HRBCs were diluted to a concentration of 2.5% in 0.15 M NaCl. From that solution, 100  $\mu$ l was mixed and incubated with both peptides, at concentrations varying from 280–2.2  $\mu$ M, for 30 min, at 37°C, followed by centrifugation as above. Then, the supernatants were collected and transferred to 96-well microtiter plates. Hemolysis (percentage) was calculated by measuring the supernatant absorbance at 414 nm using an automated absorbance microplate reader. Negative (0%) and positive (100%) hemolysis were reached by treating HRBCs with 0.15 M NaCl and 0.1% (v/v) Triton X-100, respectively. The DMSO-NaCl solution, used to resuspended peptides, was also used as control. The hemolysis was calculated by the equation:  $[(\text{Abs}_{414\text{nm}}$  of RBC treated with peptides -  $\text{Abs}_{414\text{nm}}$  HRBCs treated with 0.15 M NaCl) /  $(\text{Abs}_{414\text{nm}}$  of HRBCs treated with 0.1% TritonX-100 -  $\text{Abs}_{414\text{nm}}$  of HRBCs treated with 0.15 M NaCl)]  $\times$  100.

### 3 | RESULTS

#### 3.1 | Characterization of Mo-CBP<sub>3</sub>-Pepl and Mo-CBP<sub>3</sub>-Pepll

After synthesis, Mo-CBP<sub>3</sub>-Pepl and Mo-CBP<sub>3</sub>-Pepll were tested for purity degree by reversed-phase HPLC and by MS analysis (Figure 1). Both samples presented a chromatogram with a single sharp peak (Figure 1 inserts) with estimated purity around >95%. These RP-HPLC results were confirmed by MS analysis, which showed only one peak for Mo-CBP<sub>3</sub>-Pepl and two peaks for Mo-CBP<sub>3</sub>-Pepll (one mono-protonated and the other deprotonated peptide) (Figure 1). MS analysis revealed molecular masses of 893.25 and 1031.30 Da for Mo-CBP<sub>3</sub>-Pepl and Mo-CBP<sub>3</sub>-Pepll.

The SRCD spectra of both peptides in aqueous solution (Figure 2) presented major negative peaks centered at 198 and 202 nm for Mo-CBP<sub>3</sub>-Pepl and Mo-CBP<sub>3</sub>-Pepll, respectively (Figure 2A and 2B—black

lines). In addition, both spectra had an additional peak in the ~184-nm region. These two peaks are attributed to polypeptides with secondary structure, mainly arranged in unordered content.<sup>25</sup> Besides this, it is possible to observe only small magnitudes in the SRCD spectra for the ellipticity value at 222 nm, suggesting some minor local/partial ordering of the peptides (but not as a helix or any canonical structure).

In the presence of TFE (Figure 2A and 2B—red lines), significant changes were observed in the SRCD spectra of both peptides, which decreased the minimum at ~200 nm and increased the peak at 184 nm, together with the redshift of both peaks, indicating the acquisition of more partially ordered structures and reduction of unordered content. However, the SRCD spectra of Mo-CBP<sub>3</sub>-Pepl and Mo-CBP<sub>3</sub>-Pepll deposited on the dehydrated films (Figure 2A and 2B—blue lines) showed disorder-to-order transitions, presenting peak positioning similar to that observed for peptides in an  $\alpha$ -helix structure, with a maximum at 190 nm and two minima at ~208 and 222 nm. All these conformational changes can be attributed to the removal of water molecules from the vicinity of the peptide, forcing intrachain interactions, which resulted in better peptide ordering.<sup>26</sup>

In the presence of the zwitterionic HPS micelles, minor changes were seen in the conventional CD spectrum of Mo-CBP<sub>3</sub>-Pepl, with a small redshift of the negative peak to 203 nm, suggesting a partially ordered conformation (Figure 2C—blue line). But a more significant ordering effect occurred in Mo-CBP<sub>3</sub>-Pepl when the negatively charged SDS was employed (Figure 1C—red line). These results suggest interaction between Mo-CBP<sub>3</sub>-Pepl and the micelles. In contrast, the structure of Mo-CBP<sub>3</sub>-Pepll did not change in the presence of zwitterionic HPS micelles, and only minor changes were observed in the presence of the SDS (Figure 2D—blue and red lines). The fact of the CD spectra of Mo-CBP<sub>3</sub>-Pepll were not severely affected by the zwitterionic detergent suggests these interactions are weak, and the peptide Mo-CBP<sub>3</sub>-Pepll resides close to the aqueous environment. Indeed, the degree of hydration of the headgroup region of the HPS micelle differed from the other containing phosphocholines, with the

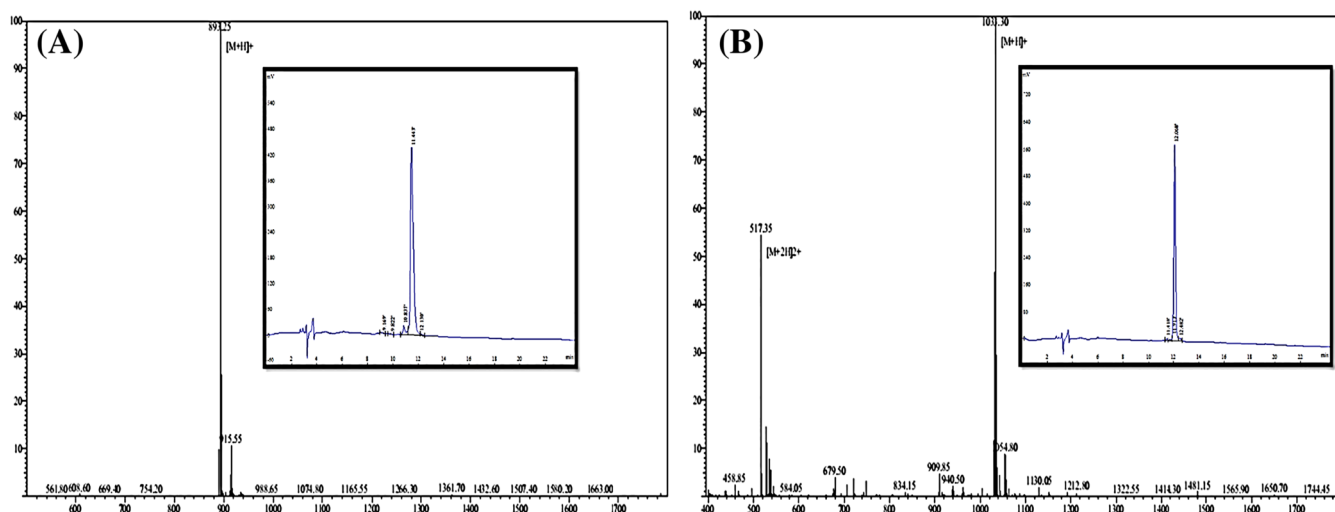


**FIGURE 1** Determination of purity of, A, Mo-CBP<sub>3</sub>-Pepl and, B, Mo-CBP<sub>3</sub>-Pepll by mass spectrometry (matrix-assisted laser desorption/ionization-time of flight [MALDI-TOF]) and reversed-phase high-performance liquid chromatography (insert)

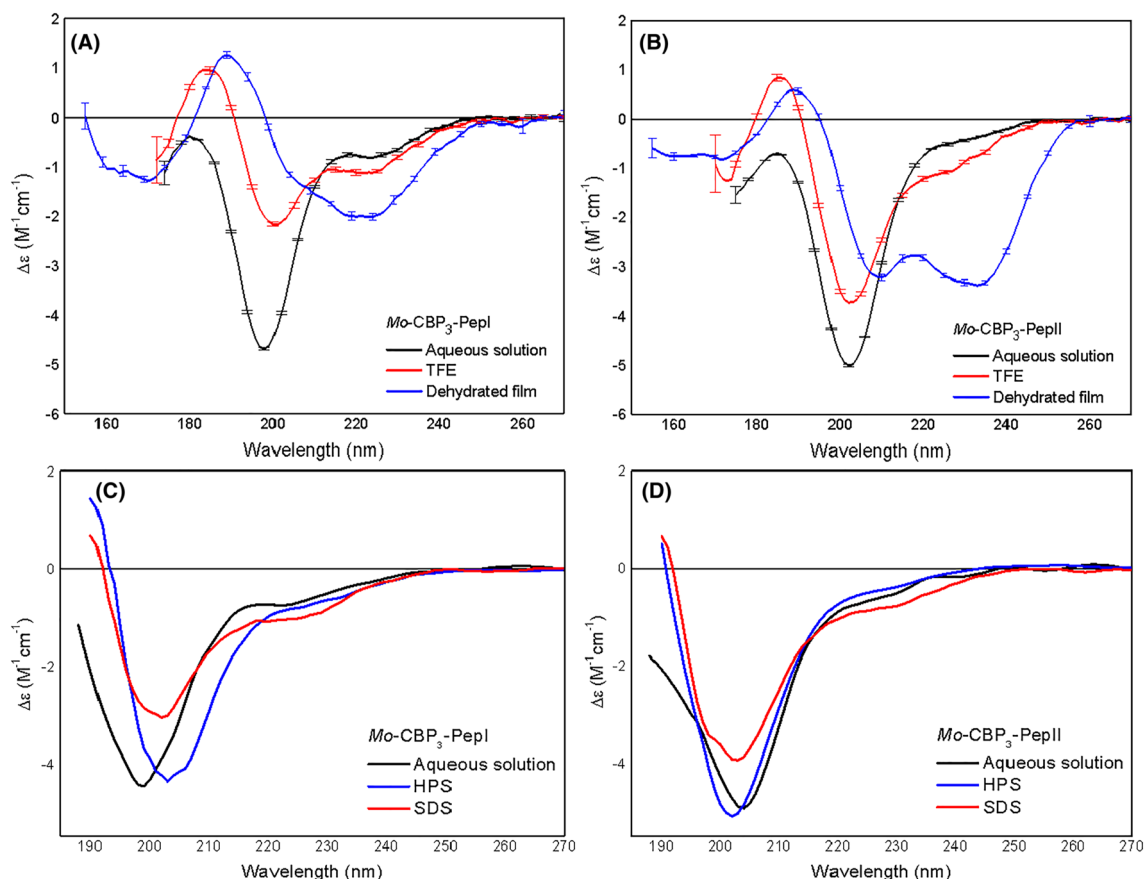


**FIGURE 2** The synchrotron radiation circular dichroism (SRCD) spectra of, A, *Mo*-CBP<sub>3</sub>-Pepl and, B, *Mo*-CBP<sub>3</sub>-PepII in aqueous solution (black), in the presence of the trifluoroethanol (TFE) (red) and in dehydrated film (blue). The conventional circular dichroism (CD) spectra of the, C, *Mo*-CBP<sub>3</sub>-Pepl and, D, *Mo*-CBP<sub>3</sub>-PepII in aqueous solution (black), or in the presence of liposomes made of surfactants *N*-hexadecyl-*N*'-dimethyl-3-ammonia-1-propane-sulfonate (HPS) (blue) or sodium dodecyl sulfate (SDS) (red). Error bars represent the standard deviation

HPS headgroup region being more hydrated than the other PC micelle. This could explain the lesser interaction in HPS.

### 3.2 | *Mo*-CBP<sub>3</sub>-Pepl and *Mo*-CBP<sub>3</sub>-PepII cause severe damage in *C. albicans* cells

SEM analyses were performed to shed light on the effects of *Mo*-CBP<sub>3</sub>-Pepl (Figure 3) and *Mo*-CBP<sub>3</sub>-PepII (Figure 4) on *C. albicans* cells. In both analyses, control cells showed spherical smooth-walled conformation, the normal shape of yeasts (Figures 2A and 3A). In contrast, *Mo*-CBP<sub>3</sub>-Pepl (Figure 3) and *Mo*-CBP<sub>3</sub>-PepII (Figure 4) induced damages in the *C. albicans* cells. The treatment with *Mo*-CBP<sub>3</sub>-Pepl resulted in cracks all over the cells, indicating damage to the cell wall (Figure 4C-H). In some *C. albicans* cells, it was possible to see the loss of cytoplasmic content (Figure 4B-C). Also, small blebs, buds, and scar buds were present in the *Mo*-CBP<sub>3</sub>-Pepl-treated cells (Figure 4B-H). The results of the treatment of *C. albicans* cells with *Mo*-CBP<sub>3</sub>-PepII (Figure 4) were very similar to those caused by *Mo*-CBP<sub>3</sub>-Pepl. However, the cracks were more evident in *Mo*-CBP<sub>3</sub>-PepII-treated cells than those treated with *Mo*-CBP<sub>3</sub>-Pepl (Figure 4C, 4D, 4F-H). In some cells, the cracks were so extensive that they covered the entire cell

surface (Figure 4C, 4D, 4G, and 4H). Small blebs, buds, and bud scars were also present in *Mo*-CBP<sub>3</sub>-PepII-treated cells (Figure 4B, 4C, 4E, and 4F). *Mo*-CBP<sub>3</sub>-PepII-treated cells also presented loss of cytoplasmic content (Figure 4H).

### 3.3 | *Mo*-CBP<sub>3</sub>-Pepl and *Mo*-CBP<sub>3</sub>-PepII resulted in membrane-pore formation

SEM analyses of *Mo*-CBP<sub>3</sub>-Pepl and *Mo*-CBP<sub>3</sub>-PepII *C. albicans* showed many cell damages (Figures 3 and 4). However, SEM results alone are not enough to show the possible pore formation in the membrane. To test the hypothesis about the induction of pore formation, *Mo*-CBP<sub>3</sub>-Pepl- and *Mo*-CBP<sub>3</sub>-PepII-treated cells were incubated with fluorescent compounds, which only can cross through damaged membranes. In the first experiment, after treatment with peptides, *C. albicans* cells were incubated with PI. PI is a compound that, once inside the cell, interacts with DNA, causing the release of red fluorescence. PI can only pass through damaged membranes. Within the cell, PI interacts with DNA. Thus, PI is an indicator of damage to the membrane. The red fluorescence produced by PI indicated the presence of pores in the membrane (Figure 5B-C), whereas in control cells (treated



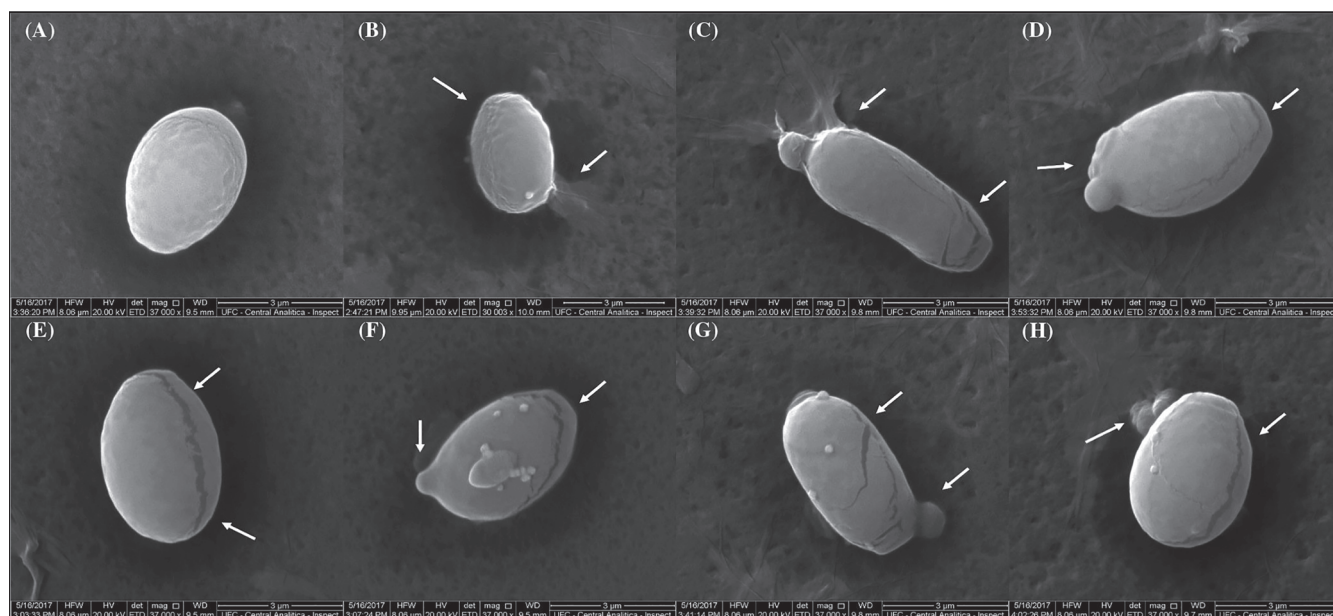


**FIGURE 3** Scanning electron microscopy (SEM) images showing alterations in the *Candida albicans* cell surface after incubation with *Mo-CBP3-PeplI*. A, The surface of untreated *C. albicans* (controls) was covered by well-defined and organized structures. B-H, Cells exposed to *Mo-CBP3-PeplI* (2.2 μM) showed considerable alterations in the shape and surface, B, F-H, with the presence of multiple buds scars; C-H, cell wall damage; B and C, and internal content loss

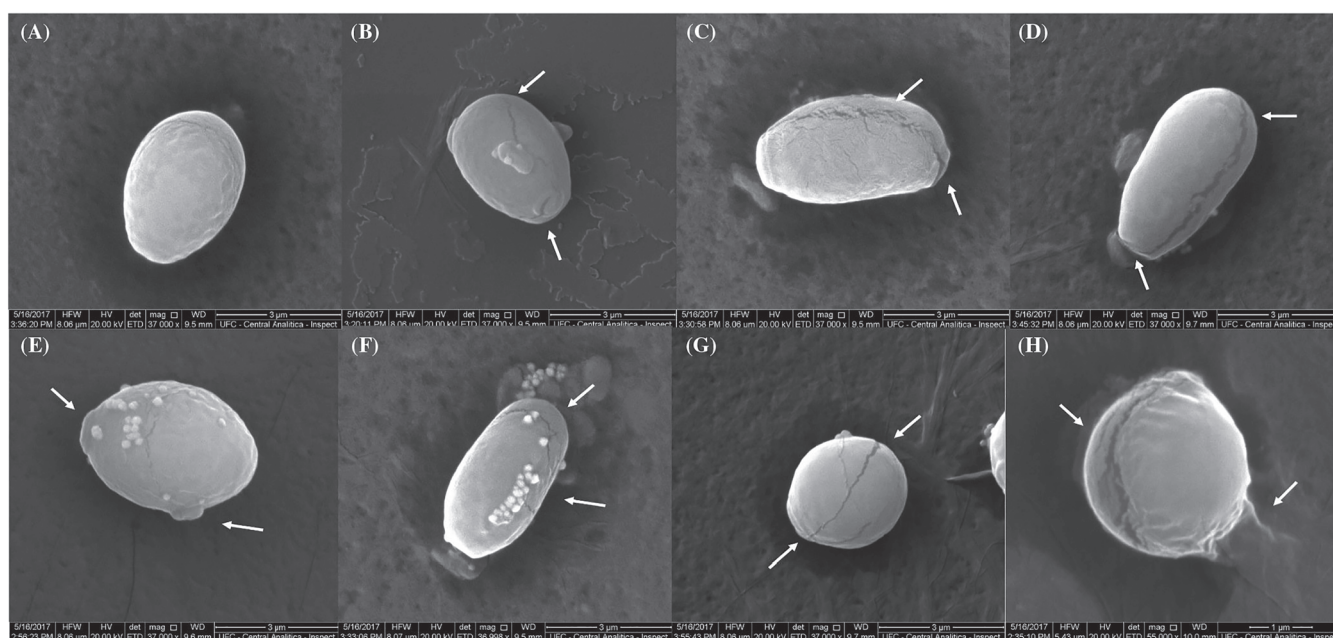


**FIGURE 4** Scanning electron microscopy (SEM) images showing alterations in the *Candida albicans* cell surface after incubation with *Mo-CBP3-PeplI*. A, The surface of untreated *C. albicans* (controls) was covered by well-defined and organized structures. B-H, Cells exposed to *Mo-CBP3-PeplI* (17.5 μM) showed considerable alterations in the cell shape and surface, B, E-F, with the presence of multiple buds and scars; C, D, F-H, cell wall damage; H, and internal content loss

with DMSO-NaCl solution), no red fluorescence was present (Figure 5A).

Furthermore, the treatment of cells with IP only indicated the presence of pores in the membrane but did not provide any information about the pore size. To obtain this information, a new experiment was conducted where cells were treated with dextrans of different

sizes conjugated with FITC (6, 10, and 20 kDa). The presence of green fluorescence in the peptide treated cells (Figure 5E-F) indicated movement of FITC-dextran through the cell membrane, different than the control cells (Figure 5D). The peptides induced the formation of different pore sizes. *Mo-CBP3-PeplI* formed pores with size  $\leq 6$  kDa (19.8 Å) (Figure 4E), while *Mo-CBP3-PeplI* showed fluorescence with the FITC-

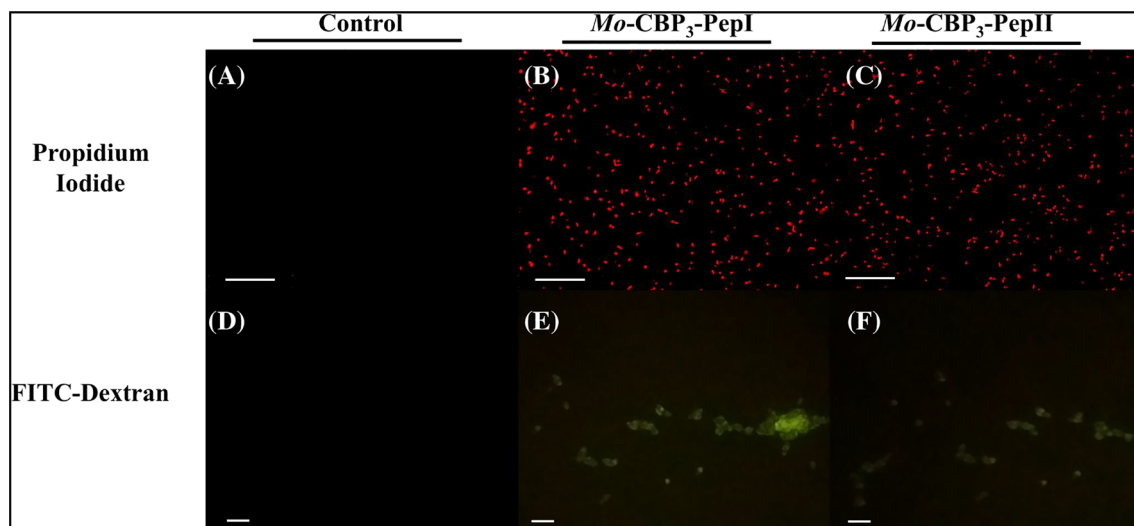


**FIGURE 5** Uptake of propidium iodide (PI) and fluorescein isothiocyanate (FITC)-dextran by *C. albicans* cells incubated with, A and D, dimethyl sulfoxide (DMSO)-NaCl; B and E, 2.2  $\mu$ M *Mo*-CBP<sub>3</sub>-PepI; C and F, or 17.5  $\mu$ M *Mo*-CBP<sub>3</sub>-PepII for 24 h, at 37 °C. Detection of red and green fluorescence in B and C and E and F indicates that cells internalized PI and FITC-dextran. A-C, bars: 200  $\mu$ m; D-F, bars: 60  $\mu$ m

dextran of 6 kDa (data not shown) and 10 kDa, indicating pore size  $\leq$ 10 kDa (Figure 5F).

In addition to pore formation, we analyzed whether or not *Mo*-CBP<sub>3</sub>-PepI and *Mo*-CBP<sub>3</sub>-PepII are able to induce ROS generation, an indicator of cell stress. The *C. albicans* cells in the control treatment (DMSO-NaCl) had no indication of ROS generation (Figure 6A and 6D), whereas both *Mo*-CBP<sub>3</sub>-PepI (Figure 6B and 6E) and *Mo*-CBP<sub>3</sub>-PepII (Figure 6C and 6F) induced ROS generation.

### 3.4 | Chitin-binding assay

Given the fact that *Mo*-CBP<sub>3</sub> is a chitin-binding protein and *C. albicans* cell walls contain chitin, we tested the ability of *Mo*-CBP<sub>3</sub>-PepI and *Mo*-CBP<sub>3</sub>-PepII to interact with chitin by using affinity chromatography. As shown in Figure 6, both peptides interacted with chitin, being eluted only after 0.1 M of acetic acid (Figure 7A) and 0.1 M of NaOH (Figure 7B) for *Mo*-CBP<sub>3</sub>-PepI and *Mo*-CBP<sub>3</sub>-PepII, respectively.

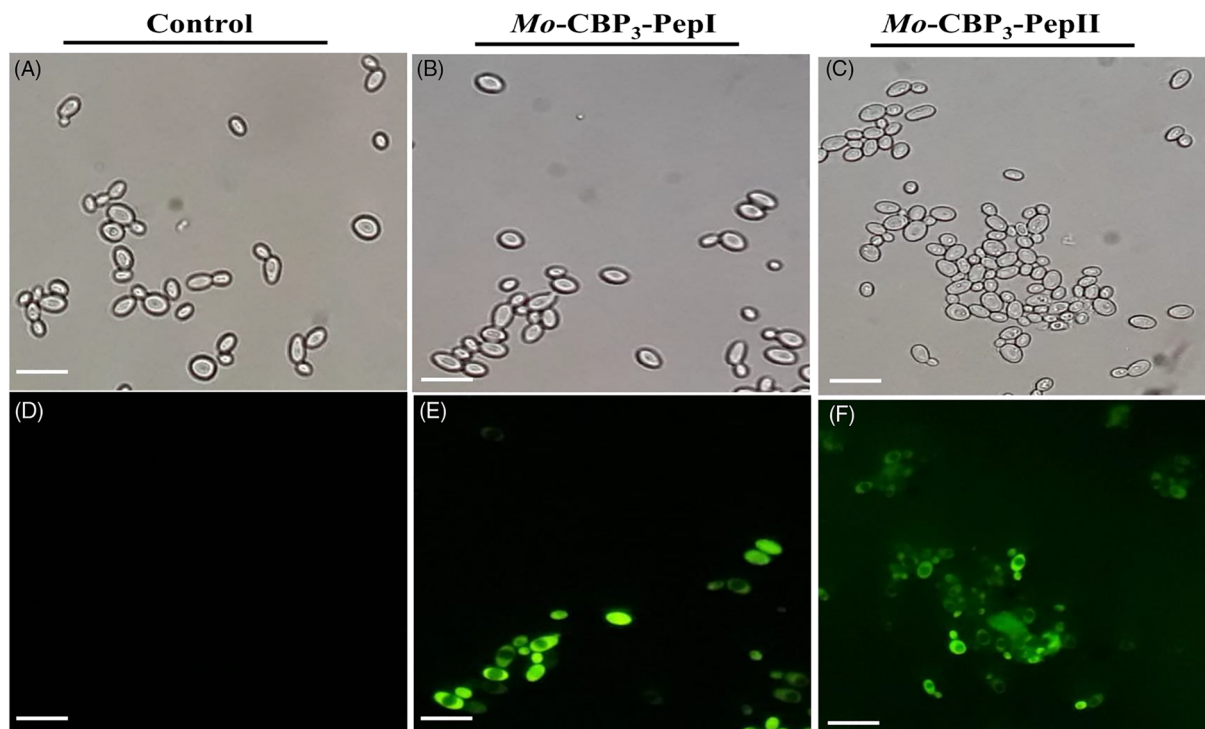


**FIGURE 6** Overproduction of reactive oxygen species (ROS) in *Candida albicans* cells induced by 2.2  $\mu$ M *Mo*-CPB<sub>3</sub>-PepI and 17.5  $\mu$ M *Mo*-CPB<sub>3</sub>-PepII. After incubation with peptides, *C. albicans* cells were treated with 2',7'-dichlorofluorescein diacetate (DCFH-DA) for 15 min at 37°C. Then, cells were visualized with an Olympus BX 60 fluorescence microscope (excitation wavelength 488 nm, emission wavelength 527 nm). A-C, Representing cells under light field and, D-F, representing cells at fluorescence filter as cited before. Bars: 500 nm

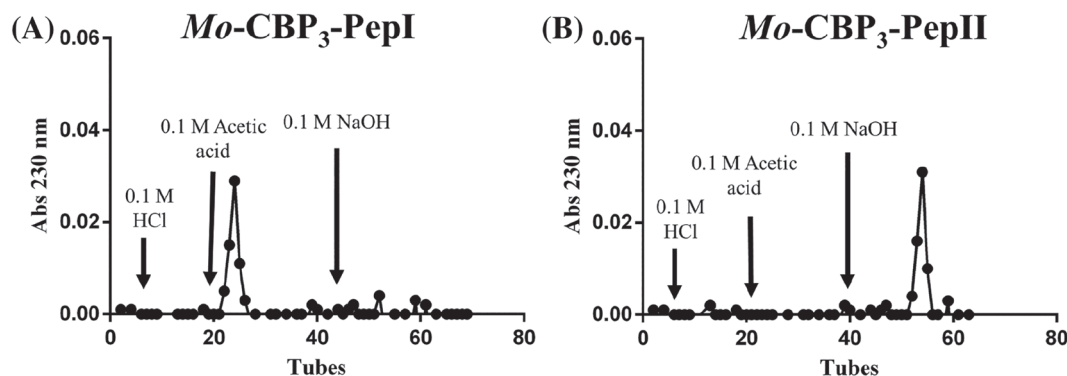


**FIGURE 7** Affinity chromatography of, A, *Mo-CBP<sub>3</sub>-PepI* and, B, *Mo-CBP<sub>3</sub>-PepII* in chitin column previously equilibrated with dimethyl sulfoxide (DMSO)-NaCl solution. The retained *Mo-CBP<sub>3</sub>-PepI* was eluted with, A, 0.1 M acetic acid and, B, *Mo-CBP<sub>3</sub>-PepII* with 0.1 M NaOH

### 3.5 | Synergistic action

The synergistic action between NYS and *Mo-CBP<sub>3</sub>-PepI* or *Mo-CBP<sub>3</sub>-PepII* reduced the NYS and peptide concentration needed to attain  $IC_{90}$  for *C. albicans*. The  $IC_{90}$  values of *Mo-CBP<sub>3</sub>-PepI* and *Mo-CBP<sub>3</sub>-PepII* combined with NYS declined from 2.2  $\mu$ M to 0.18  $\mu$ M and 17.5  $\mu$ M to 2.18  $\mu$ M, respectively (Table 1). Likewise, the  $IC_{90}$  of NYS decreased from 108  $\mu$ M (alone) to 0.16  $\mu$ M when combined with *Mo-CBP<sub>3</sub>-PepI* or *Mo-CBP<sub>3</sub>-PepII*, reducing 666 times the concentration to reach the  $IC_{90}$  (Table 1). These changes generated a FICI value of 0.13. Values below 0.5 indicate a synergistic effect (Table 1).

### 3.6 | Toxicity to human red blood cells

To obtain information about the applicability of peptides, the toxicity to HRBCs was assayed. There was no indication of toxicity of *Mo-CBP<sub>3</sub>-PepI* to any type of HRBC, even at concentrations 30 and 120 times higher than the  $MIC_{90}$  (Figure 8). In turn, for *Mo-CBP<sub>3</sub>-PepII*, the concentrations tested were 4 and 16 times higher than the  $MIC_{90}$ . *Mo-CBP<sub>3</sub>-PepII* only showed slight hemolytic effect against type B HRBCs at a concentration 16 times higher than the  $MIC_{90}$  (Figure 8).

## 4 | DISCUSSION

*C. albicans* is a serious threat to human health worldwide. As an opportunistic pathogen, it can cause bloodstream infection, and in some cases death. Among patients who develop untreatable infection by *Candida* species are immunocompromised, HIV positive, and intensive care unit patients.<sup>8,9</sup> The emergence of drug-resistant *Candida* species makes this scenario worse. Thus, the search for and development of new drugs to treat these infections are imperative to improve patients' chance to survive.<sup>1-3</sup>

In this respect, natural AMPs are promising molecules, either as substitutes or adjuvants in these treatments. However, they have some disadvantages for the development of new drugs, such

as high toxicity, low resistance to proteolysis, and high cost of purification. The development of SAMPs is an alternative solution to this problem.<sup>11-13</sup> Bioinspired SAMPs using natural AMPs can bring the best features of the molecules with very low or even no toxicity.<sup>27,28</sup> For example, the synthetic peptide LAH4 presented higher activity against *Escherichia coli* and *Staphylococcus aureus* than natural peptide Magainin 2, which was used as a model to design LAH4.<sup>29,30</sup> Recently, our research group designed three peptides from the antifungal protein *Mo-CBP<sub>3</sub>*. Among those peptides, *Mo-CBP<sub>3</sub>-PepI* and *Mo-CBP<sub>3</sub>-PepII* presented anticandidal activity.<sup>13</sup> In this study, the mechanism behind this activity was evaluated to understand how these peptides work and their possible applications.

The  $IC_{90}$  values of *Mo-CBP<sub>3</sub>-PepI* and *Mo-CBP<sub>3</sub>-PepII* against *C. albicans* were 2.2 and 17.5  $\mu$ M, respectively. This difference is likely because *Mo-CBP<sub>3</sub>-PepI* can alter its secondary structure (Figure 2C) when interacting with the membrane, improving the interaction and pore formation, thus enhancing its activity. It is already known that peptides can change their secondary structures to  $\alpha$ -helix to improve interaction with membranes. A thermodynamic study performed by Wieprecht et al.<sup>31</sup> revealed that the peptide magainin 2 increases its helicity upon membrane interaction. The authors concluded that the helix formation generates a necessary and strong driving force to peptide insertion in the membrane.<sup>31</sup> Such conformational changes in the *Mo-CBP<sub>3</sub>-PepI* structure allowed it to bind to the two model membranes employed, regardless of their net surface charge. Thus, *Mo-CBP<sub>3</sub>-PepI* was 7.9 times more active than *Mo-CBP<sub>3</sub>-PepII*. These findings probably explain the stronger inhibitory action of *Mo-CBP<sub>3</sub>-PepI* on *C. albicans* compared with *Mo-CBP<sub>3</sub>-PepII*. Accordingly, several antimicrobial peptides are able to change their secondary structure to  $\alpha$ -helical conformation upon interaction with target membranes, enhancing the interaction.<sup>32</sup> In addition to conformational changes, the sequence of both peptides helps in the interaction with the membrane. The presence of an arginine residue is essential to confer a positive charge, which is involved in the ionic interaction with the negatively charged membrane of *C. albicans* cells. The presence of proline residues in peptides has been related to their interaction with microbial membranes. For instance, Buforin II is a potent



**TABLE 1** Combined effect of Mo-CBP<sub>3</sub>-Pepl and Mo-CBP<sub>3</sub>-Pepll and nystatin (NYS)

Strain	IC <sub>50</sub> <sup>aa</sup> (μM)				FICI <sup>bb</sup>			
	Only	Combination	Interpretation	Only	Combination	Interpretation	FICI <sup>bb</sup>	
<i>C. albicans</i> ATCC 10231	NYS	Mo-CBP <sub>3</sub> -Pepl		NYS	Mo-CBP <sub>3</sub> -Pepl		0.13	
	108	2.2		108	0.16	0.27	0.13	

Abbreviation: American Type Culture Collection.

<sup>a</sup>IC<sub>50</sub>: Concentration that inhibited yeast growth by 90%.<sup>b</sup>FICI: Fractional inhibitory concentration index. FICI values suggest antagonistic (FICI >4.0), indifferent (FICI >0.5–4.0) and synergistic (FICI ≤0.5) effect.

antimicrobial peptide that has a proline residue essential to its activity. Mutations in Buforin II, replacing the proline, result in loss of Buforin II activity, suggesting the importance of proline for antimicrobial activity.<sup>33</sup> Related to cysteine residue content, PyMol analysis revealed that those cysteine residues were not involved in the disulfide bridge. Although the mechanism is unclear, it is known that somehow cysteine contributes to antimicrobial activity. For example, Schroeder et al.<sup>34</sup> showed that the treatment of the peptide human beta-defensin-1 (hDB-1) with dithiothreitol (DTT) reduced disulfide bridges, leading to free cysteine residues and increasing antimicrobial activity. In addition, replacing the cysteine residues in hDB-1 by alanine from serine residues reduced hDB-1 antimicrobial activity. These results suggest, although unclear, the importance of cysteine residues to antimicrobial activity.

The results suggest that Mo-CBP<sub>3</sub>-Pepl and Mo-CBP<sub>3</sub>-Pepll were able to break the cell wall and induce membrane-pore formation, leading to loss of cell content of *C. albicans* (Figures 3 and 4). Compared with VS2 and VS3 (two SAMPs designed by Maurya et al.<sup>22</sup>), the activities presented here are 35 and 17 times higher for Mo-CBP<sub>3</sub>-Pepl and 4.5 and 3 higher for Mo-CBP<sub>3</sub>-Pepll. Also, SEM analysis revealed that the damage caused in *C. albicans* cells by Mo-CBP<sub>3</sub>-Pepl and Mo-CBP<sub>3</sub>-Pepll was more evident compared with VS2 and VS3.

Unlike the common drugs used to treat infection, which have a specific target (i.e., protein involved in cell wall synthesis), most SAMPs target cell membranes, leading to pore formation or damage to the cell wall.<sup>13,22</sup> This makes it hard for the microorganism to develop resistance, because it has to change the membrane or cell wall composition, which has a high metabolic cost.<sup>35</sup> The pore formation in *C. albicans* membranes induced by Mo-CBP<sub>3</sub>-Pepl and Mo-CBP<sub>3</sub>-Pepll was clear (Figure 5A–C). Interestingly, Mo-CBP<sub>3</sub>-Pepl and Mo-CBP<sub>3</sub>-Pepll presented different behaviors when interacting with *C. albicans* cell membranes. Mo-CBP<sub>3</sub>-Pepl interacted by forming pore sizes of 6 kDa (Figure 5D) and Mo-CBP<sub>3</sub>-Pepll of 10 kDa (Figure 5F). These results are very interesting because Mo-CBP<sub>3</sub>-Pepl and Mo-CBP<sub>3</sub>-Pepll have sizes of 893.10 and 1033.23 Da, respectively (Figure 1). Therefore, we suggest that the pore formation demonstrated is due to self-association after membrane insertion. This is an important feature for SAMPs responsible for pore formation in membranes.<sup>36,37</sup> Our results related to pore formation suggest the existence of a barrel-stave mechanism employed by peptides to induce pores. In this mechanism, peptide-lipid interaction occurs first, and then inside the membrane peptide-peptide interaction occurs, leading to the formation of stable pores in the membranes.<sup>36–38</sup> By comparing the sizes of Mo-CBP<sub>3</sub>-Pepl and Mo-CBP<sub>3</sub>-Pepll and the pores formed, it can be hypothesized that Mo-CBP<sub>3</sub>-Pepl and Mo-CBP<sub>3</sub>-Pepll move through those pores to reach intracellular targets. If so, the peptides may be internalized by energy-independent pathways, known as direct translocation through the pores formed.<sup>17,39</sup> Once inside the cells, peptides can inhibit many cytoplasmic processes, such as cell wall synthesis, protein synthesis, and folding.<sup>37</sup> Maurya et al.<sup>22</sup> described the ability of VS2 and VS3 to form pores in the membrane of *C. albicans* and pass through those pores to reach some targets inside the cell.

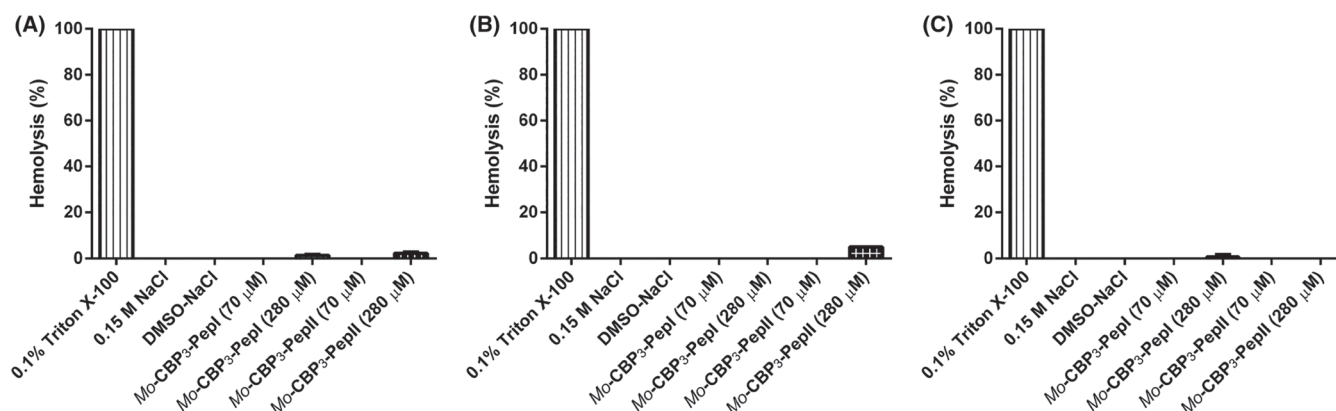


**FIGURE 8** Effect of *Mo*-CBP<sub>3</sub>-Pepl and *Mo*-CBP<sub>3</sub>-PeplII on human red blood cells. *Mo*-CBP<sub>3</sub>-Pepl and *Mo*-CBP<sub>3</sub>-PeplII concentrations used for incubation were 30 and 120, and were 4 and 16 times higher than MIC<sub>90</sub>, respectively, against A type-A, B type-B, and C type-O of human red blood cells

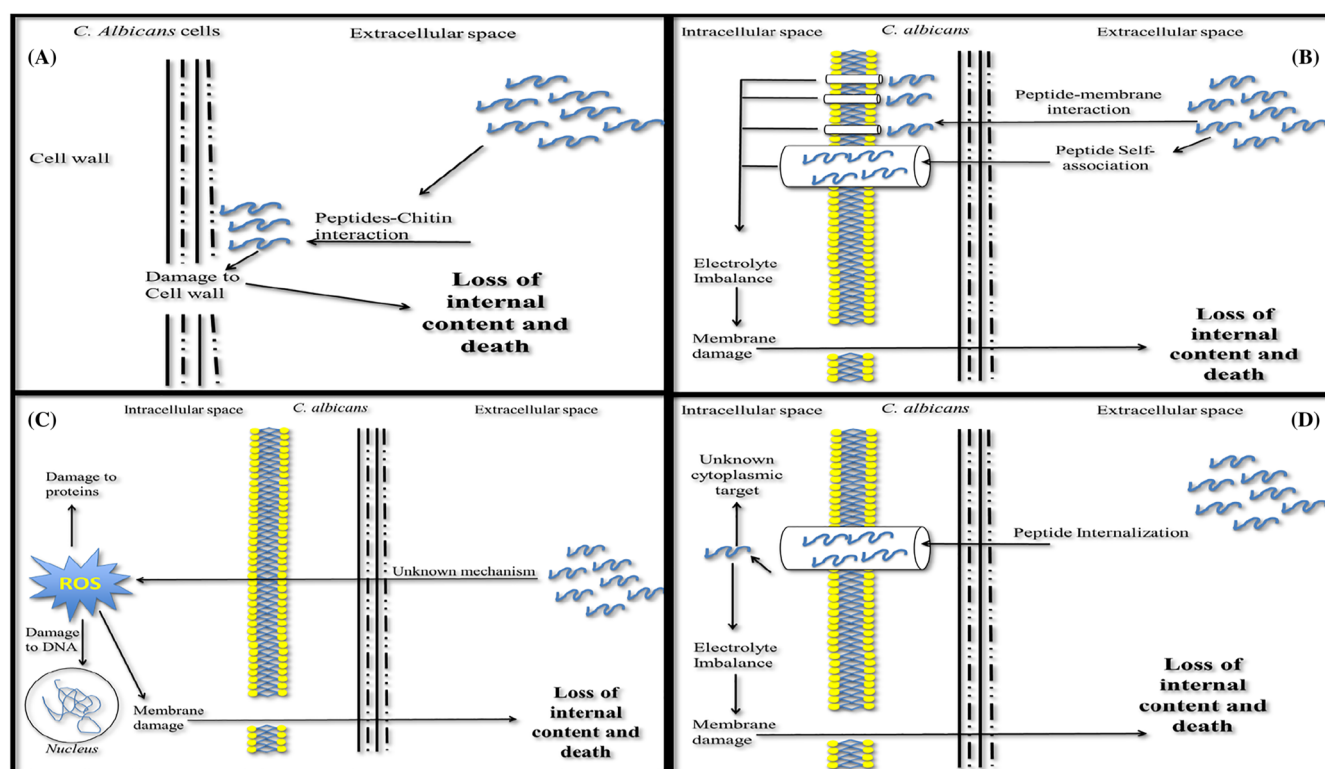


**FIGURE 9** Diagrams indicating all possible mechanisms for anticandidal activity of *Mo*-CBP<sub>3</sub>-Pepl and *Mo*-CBP<sub>3</sub>-PeplII: A, chitin interaction leading to broken cell wall; B, pore formation in the membrane inducing damage, electrolyte imbalance, and loss of internal content; C, inducement of reactive oxygen species (ROS) overproduction, which can damage many intracellular components; and, D, penetration of peptides through the membrane to reach intracellular targets

In addition, chitin is a very important component in the fungal cell wall, making it an important target of SAMPs.<sup>40,41</sup> *Mo*-CBP<sub>3</sub> has strong antifungal activity against phytopathogenic fungi, which have chitin in the cell wall. Contrarily, it does not present any activity against oomycetes, which have no chitin in the cell wall. It is clear that the antifungal action of *Mo*-CBP<sub>3</sub> depends on interaction with chitin.<sup>23</sup> Here, both peptides were able to bind to chitin (Figure 7). Likewise, Rogozhin et al.<sup>42</sup> reported a chitin-binding SmAMP3 (*Stellaria media* antimicrobial peptide 3), which displayed high antifungal activity

compared with SmAMP1.1a, because the latter did not interact with chitin. Contrary to our case, SmAMP3 is a hevein-derived peptide, which explains its interaction with chitin.<sup>42</sup> In contrast, the peptides reported here do not possess a hevein-like domain involved in chitin interaction by many chitin-binding proteins. However, our results indicate that the chitin column was previously equilibrated with the 0.5 M NaCl solution, suggesting that the observed interaction was supported by strong ionic interactions between the peptides and the chitin matrix.

Thus, this interaction might be involved with the demonstrated anticandidal activity of both peptides. This finding suggests that the chitin present in the fungal cell wall might be one of the potential targets to which *Mo*-CBP<sub>3</sub>-Pepl and *Mo*-CBP<sub>3</sub>-Pepll bind and begin their deleterious action in the microorganism. Probably this interaction also explains the ability of *Mo*-CBP<sub>3</sub>-Pepl and *Mo*-CBP<sub>3</sub>-Pepll to induce many damages to *C. albicans* cell walls, rupturing them and leading to cell death, as shown by SEM analysis (Figures 3 and 4).

Furthermore, *Mo*-CBP<sub>3</sub>-Pepl and *Mo*-CBP<sub>3</sub>-Pepll induced ROS overproduction in *C. albicans* (Figure 6E-F), leading to cell death.<sup>13,41,43</sup> Similar to other peptides,<sup>15,43,44</sup> the mechanism involved in ROS overproduction induced by *Mo*-CBP<sub>3</sub>-Pepl and *Mo*-CBP<sub>3</sub>-Pepll is unclear. Nonetheless, it is known that ROS can damage important molecules such as proteins, DNA, and lipids, killing the cell.<sup>13,22</sup> Regarding the damage to DNA or RNA molecules, it has been reported that some synthetic peptides interact and damage cell DNA or RNA or impair small interfering RNA (siRNA) functions, leading the cell to death.<sup>45</sup> Here, bioinformatics and in vitro analysis showed that neither *Mo*-CBP<sub>3</sub>-Pepl nor *Mo*-CBP<sub>3</sub>-Pepll were able to cause damage to cellular nucleic acids of any kind (data not shown).

Regarding the clinical application, *Mo*-CBP<sub>3</sub>-Pepl and *Mo*-CBP<sub>3</sub>-Pepll had no hemolytic activity against type A, B, and O human erythrocytes, even at concentrations 30 and 120, and were 4 and 16 times higher than the IC<sub>90</sub> values against *C. albicans*, respectively (Figure 8). Many current therapies are based on drug combinations, employing two or more drugs with different modes of action, which can improve the antimicrobial treatment. In addition, this combination can reduce toxic effects and the cost of treatments.<sup>46</sup> Also, many peptides from natural sources have shown synergistic activity with conventional drugs against fungi. Studies of this type using SAMPs are very limited. For instance, Harries and Coote<sup>46</sup> tested 6,752 cyclic synthetic peptides, which showed no synergistic activity with caspofungin and/or anidulafungin against *C. albicans* isolates.

Another clinical application of peptides could be as adjuvants. As summarized in Table 1, *Mo*-CBP<sub>3</sub>-Pepl and *Mo*-CBP<sub>3</sub>-Pepll improved the activity of NYS by synergistic action. To achieve the IC<sub>90</sub> against *C. albicans*, in the presence of either *Mo*-CBP<sub>3</sub>-Pepl or *Mo*-CBP<sub>3</sub>-Pepll, required a concentration of NYS 666 times lower than NYS alone. The FICI values of NYS and *Mo*-CBP<sub>3</sub>-Pepl or *Mo*-CBP<sub>3</sub>-Pepll were ≤ 0.5 (0.13, Table 1). NYS (polyene) promotes anticandidal activity by interacting with ergosterol in the fungal cell membrane, which makes it a very efficient drug for the treatment of skin infections caused by *Candida* sp. However, NYS is very toxic due to the high hemolytic activity against human blood, limiting its application. In this respect, our results about the synergistic effect are important, because NYS can be administered at very low concentrations while maintaining high activity with no collateral effect.

Figure 9 summarizes all the possible mechanisms of anticandidal activity of *Mo*-CBP<sub>3</sub>-Pepl and *Mo*-CBP<sub>3</sub>-Pepll: (1) chitin interaction leading to cell wall rupture (Figure 9A); (2) pore formation in the membrane, inducing loss of internal content (Figure 9B); (3) inducement of ROS overproduction, which can damage many intracellular components (Figure 9C); and (4) passage of the peptides through the

membrane to reach some cytoplasmic targets (Figure 9D). Altogether, these mechanisms explain the potent anticandidal activity of *Mo*-CBP<sub>3</sub>-Pepl and *Mo*-CBP<sub>3</sub>-Pepll. In addition, our data about membrane-pore sizes (Figure 5E-F) along with data published in the literature<sup>17,22,36</sup> suggest that *Mo*-CBP<sub>3</sub>-Pepl and *Mo*-CBP<sub>3</sub>-Pepll can move through the membrane and reach cytoplasmic targets, enhancing their action against *C. albicans* (Figure 9D).

## 5 | CONCLUSION

Based on the strong anticandidal activity, absence of toxic effects, and synergistic effect, enhancing the antifungal activity of NYS, we suggest that *Mo*-CBP<sub>3</sub>-Pepl and *Mo*-CBP<sub>3</sub>-Pepll are promising peptides either as new antimicrobial agents for clinical applications or adjuvants of conventional drugs because of their high activity and low toxicity.

## ACKNOWLEDGEMENTS

This study was supported by the CNPq (National Council for Scientific and Technological Development), process numbers 308107/2013-6 and 306202/2017-4), Coordenação de Aperfeiçoamento de Pessoal de Nível Superior – National Institute of Science and Technology of Bioinspiration (Process Number: 465507/2014-0) and the São Paulo State Research Foundation (FAPESP, grant no. 2018/19546-7 to JLSL). We are grateful to the central analytical facilities at UFC, Brazil, and the staff of the ASTRID2 synchrotron (Aarhus, Denmark) for access to the AU-CD beamline by JLSL.

## CONFLICT OF INTEREST

All authors declare no conflict of interest.

## AUTHOR CONTRIBUTIONS

All authors made substantial contributions in the following steps: (1) the conception and design of the study, or acquisition of data or analysis and interpretation of data, were done by PFNS, JTAO, PGL, IMV, LPD, and JXSN; (2) drafting the article or revising it critically for important intellectual content was done by PFNS, DOBS, and CDTF; and (3) final approval of the version to be submitted was done by PFNS and CDTF.

## ETHICAL APPROVAL

None sought.

## ORCID

Pedro F.N. Souza  <https://orcid.org/0000-0003-2524-4434>

## REFERENCES

- Centers for Disease Control. Antibiotic resistance threats in the United States 2013.
- World Health Organization. Antimicrobial resistance: global report on surveillance; 2015.

3. Laxminarayan R, Duse A, Wattal C, et al. Antibiotic resistance-the need for global solutions. *Lancet Infect Dis*. 2013;13(12):1057-1098. [https://doi.org/10.1016/S1473-3099\(13\)70318-9](https://doi.org/10.1016/S1473-3099(13)70318-9)
4. Holmes AH, Moore LSP, Sundsfjord A, et al. Understanding the mechanisms and drivers of antimicrobial resistance. *Lancet*. 2016;387(10014):176-187. [https://doi.org/10.1016/S0140-6736\(15\)00473-0](https://doi.org/10.1016/S0140-6736(15)00473-0)
5. Cowen LE, Sanglard D, Howard SJ, Rogers PD, Perlin DS. Mechanisms of antifungal drug resistance. *Cold Spring Harb Perspect Med*. 2014;5(7):1-23. <https://doi.org/10.1101/cshperspect.a019752>
6. Brown GD, Denning DW, Gow NAR, Levitz SM, Netea MG, White TC. Hidden killers: human fungal infections. *Sci Transl Med*. 2012;4(165):165-180. <https://doi.org/10.1126/scitranslmed.3004404>
7. Sanguinetti M, Posteraro B, Lass-Flörl C. Antifungal drug resistance among *Candida* species: mechanisms and clinical impact. *Mycoses*. 2015;58:2-13. <https://doi.org/10.1111/myc.12330>
8. Morgan J, Meltzer MI, Plikaytis BD, et al. Excess mortality, hospital stay, and cost due to Candidemia: a case-control study using data from population-based Candidemia surveillance. *Infect Control Hosp Epidemiol*. 2005;26(06):540-547. <https://doi.org/10.1086/502581>
9. Antinori S, Milazzo L, Sollima S, Galli M, Corbellino M. Narrative Review Candidemia and Invasive Candidiasis in Adults: A Narrative Review. *European Journal of Internal Medicine*. 2016;34:21-28. <https://doi.org/10.1016/j.ejim.2016.06.029>
10. Fu J, Ding Y, Wei B, et al. Epidemiology of *Candida albicans* and non-*C. albicans* of neonatal Candidemia at a tertiary care hospital in western China. *BMC Infect Dis*. 2017;17(1):329-341. <https://doi.org/10.1186/s12879-017-2423-8>
11. Mohamed MF, Abdelkhalik A, Seleem MN. Evaluation of short synthetic antimicrobial peptides for treatment of drug-resistant and intracellular staphylococcus Aureus. *Sci Rep*. 2016;6(1):29707-29721. <https://doi.org/10.1038/srep29707>
12. Ghosh C, Haldar J. Membrane-active small molecules: designs inspired by antimicrobial peptides. *ChemMedChem*. 2015;10(10):1606-1624. <https://doi.org/10.1002/cmdc.201500299>
13. Oliveira JTA, Souza PFN, Vasconcelos IM, et al. Mo-CBP3-Pepl, Mo-CBP3-PeplI, and Mo-CBP3-PeplII are synthetic antimicrobial peptides active against human pathogens by stimulating ROS generation and increasing plasma membrane permeability. *Biochimie*. 2019;157:10-21. <https://doi.org/10.1016/j.bjochi.2018.10.016>
14. Dias LP, Souza PFN, Oliveira JTA, et al. RcAlb-PeplI, a synthetic small peptide bioinspired in the 2S albumin from the seed cake of *Ricinus communis*, is a potent antimicrobial agent against *Klebsiella pneumoniae* and *Candida parapsilosis*. *Biochim Biophys Acta - Biomembr*. 2019;1862(2):183092-183103. <https://doi.org/10.1016/j.bbamem.2019.183092>
15. Lopes FES, da Costa HPS, Souza PFN, et al. Peptide from thaumatin plant protein exhibits selective anticandidal activity by inducing apoptosis via membrane receptor. *Phytochemistry*. 2019;159:46-55. <https://doi.org/10.1016/j.phytochem.2018.12.006>
16. Souza PFN, Vasconcelos IM, Silva FDA, et al. A 2S albumin from the seed cake of *Ricinus communis* inhibits trypsin and has strong antibacterial activity against human pathogenic bacteria. *J Nat Prod*. 2016;79(10):2423-2431. <https://doi.org/10.1021/acs.jnatprod.5b01096>
17. Deshayes S, Heitz A, Morris MC, Charnet P, Divita G, Heitz F. Insight into the mechanism of internalization of the cell-penetrating carrier peptide Pep-1 through conformational analysis <sup>†</sup>. *Biochemistry*. 2004;43(6):1449-1457. <https://doi.org/10.1021/bi035682s>
18. da Cruz WT, Bezerra EHS, Grangeiro TB, et al. Structural and enzymatic characterization of Peruvianin-I, the first germin-like protein with proteolytic activity. *Int J Biol Macromol*. 2019;126:1167-1176. <https://doi.org/10.1016/j.IJBIOMAC.2019.01.023>
19. Miles AJ, Wallace BA. CDtoolX, a downloadable software package for processing and analyses of circular dichroism spectroscopic data. *Protein Sci*. 2018;27(9):1717-1722. <https://doi.org/10.1002/pro.3474>
20. Neto JXS, Pereira ML, Oliveira JTA, et al. A chitin-binding protein purified from *Moringa Oleifera* seeds presents Anticandidal activity by increasing cell membrane permeability and reactive oxygen species production. *Front Microbiol*. 2017;8:980-992. <https://doi.org/10.3389/fmicb.2017.00980>
21. Clinical and Laboratory Standards Institute. M27-A3: Reference method for broth dilution antifungal susceptibility testing of yeasts; approved standard—third edition. 2008.
22. Maurya IK, Pathak S, Sharma M, et al. Antifungal activity of novel synthetic peptides by accumulation of reactive oxygen species (ROS) and disruption of cell wall against *Candida albicans*. *Peptides*. 2011;32(8):1732-1740. <https://doi.org/10.1016/J.PEPTIDES.2011.06.003>
23. Gifoni JM, Oliveira JTA, Oliveira HD, et al. A novel chitin-binding protein from *Moringa oleifera* seed with potential for plant disease control. *Biopolymers*. 2012;98(4):406-415. <https://doi.org/10.1002/bip.22068>
24. Lu M, Yu C, Cui X, Shi J, Yuan L, Sun S. Gentamicin synergises with azoles against drug-resistant *Candida albicans*. *Int J Antimicrob Agents*. 2018;51(1):107-114. <https://doi.org/10.1016/J.IJANTIMICAG.2017.09.012>
25. Kumagai PS, DeMarco R, Lopes JLS. Advantages of synchrotron radiation circular dichroism spectroscopy to study intrinsically disordered proteins. *Eur Biophys J*. 2017;46(7):599-606. <https://doi.org/10.1007/s00249-017-1202-1>
26. Cammers-Goodwin A, Allen TJ, Oslick SL, McClure KF, Lee JH, Kemp DS. Mechanism of stabilization of helical conformations of polypeptides by water containing trifluoroethanol. *J Am Chem Soc*. 1996;118(13):3082-3090. <https://doi.org/10.1021/ja952900z>
27. Lata S, Sharma BK, Raghava GPS. Analysis and prediction of antibacterial peptides. *BMC Bioinformatics*. 2007;8(1):263-273. <https://doi.org/10.1186/1471-2105-8-263>
28. Lata S, Mishra NK, Raghava GP. AntiBP2: improved version of antibacterial peptide prediction. *BMC Bioinformatics*. 2010;11(Suppl 1):1-7. <https://doi.org/10.1186/1471-2105-11-S1-S19>
29. Mason AJ, Gasnier C, Kichler A, et al. Enhanced membrane disruption and Antibiotic action against pathogenic bacteria by designed histidine-rich peptides at acidic pH. *Antimicrob Agents Chemother*. 2006;50(10):3305-3311. <https://doi.org/10.1128/AAC.00490-06>
30. James Mason A, Moussaoui W, Abdelrahman T, et al. Structural determinants of antimicrobial and antiparasitic activity and selectivity in histidine-rich amphipathic cationic peptides. *J Biol Chem*. 2009;284(1):119-133. <https://doi.org/10.1074/jbc.M806201200>
31. Wieprecht T, Apostolov O, Beyermann M, Seelig J. Thermodynamics of the  $\alpha$ -helix-coil transition of amphipathic peptides in a membrane environment: implications for the peptide-membrane binding equilibrium. *J Mol Biol*. 1999;294(3):785-794. <https://doi.org/10.1006/jmbi.1999.3268>
32. Sato H, Feix JB. Peptide-membrane interactions and mechanisms of membrane destruction by amphipathic  $\alpha$ -helical antimicrobial peptides. *Biochim Biophys Acta - Biomembr*. 2006;1758(9):1245-1256. <https://doi.org/10.1016/j.bbamem.2006.02.021>
33. Xie Y, Fleming E, Chen JL, Elmore DE. Effect of proline position on the antimicrobial mechanism of buforin II. *Peptides*. 2011;32(4):677-682. <https://doi.org/10.1016/j.peptides.2011.01.010>
34. Schroeder BO, Wu Z, Nuding S, et al. Reduction of disulphide bonds unmasks potent antimicrobial activity of human  $\beta$  2-defensin 1. *Nature*. 2011;469(7330):419-423. <https://doi.org/10.1038/nature09674>
35. Dong N, Zhu X, Chou S, Shan A, Li W, Jiang J. Antimicrobial potency and selectivity of simplified symmetric-end peptides. *Biomaterials*. 2014;35(27):8028-8039. <https://doi.org/10.1016/j.biomaterials.2014.06.005>



36. Splith K, and Neundorff, I., 2011. Antimicrobial peptides with cell-penetrating peptide properties and vice versa. *European Biophysics Journal*, 40(4), pp.387-397. <https://doi.org/10.1007/s00249-011-0682-7>.
37. Huang Y, Huang J, Chen Y. Alpha-helical cationic antimicrobial peptides: relationships of structure and function. *Protein & Cell*. 2010; 1(2):143-152. <https://doi.org/10.1007/s13238-010-0004-3>.
38. Bechinger B, Gorr S-U. Antimicrobial peptides: mechanisms of action and resistance. *J Dent Res*. 2017;96(3):254-260. <https://doi.org/10.1177/0022034516679973>
39. Simeoni F, Morris MC, Heitz F, Divita G. Insight into the mechanism of the peptide-based gene delivery system MPG: implications for delivery of siRNA into mammalian cells. *Nucleic Acids Res*. 2003; 31(11):2717-2724.
40. Batista AB, Oliveira JTA, Gifoni JM, et al. New insights into the structure and mode of action of Mo-CBP3, an antifungal chitin-binding protein of *Moringa oleifera* seeds. *PLoS One*. 2014;9(10):e111427-111436. <https://doi.org/10.1371/journal.pone.0111427>
41. Wang K, Dang W, Xie J, et al. Antimicrobial peptide protonection disturbs the membrane integrity and induces ROS production in yeast cells. *Biochim Biophys Acta - Biomembr*. 2015;1848(10):2365-2373. <https://doi.org/10.1016/j.BBAMEM.2015.07.008>
42. Rogozhin EA, Slezina MP, Slavokhotova AA, et al. A novel antifungal peptide from leaves of the weed *Stellaria media* L. *Biochimie*. 2015; 116:125-132. <https://doi.org/10.1016/j.biochi.2015.07.014>
43. Helmerhorst EJ, Troxler RF, Oppenheim FG. The human salivary peptide histatin 5 exerts its antifungal activity through the formation of reactive oxygen species. *Proc Natl Acad Sci U S A*. 2001;98(25):14637-14642. <https://doi.org/10.1073/PNAS.141366998>
44. Lee J, Lee DG. Antimicrobial peptides (AMPs) with dual mechanisms: membrane disruption and apoptosis. *J Microbiol Biotechnol*. 2015; 25(6):759-764. <https://doi.org/10.4014/jmb.1411.11058>
45. Moulay G, Leborgne C, Mason AJ, Aisenbrey C, Kichler A, Bechinger B. Histidine-rich designer peptides of the LAH4 family promote cell delivery of a multitude of cargo. *J Pept Sci*. 2017;23(4):320-328. <https://doi.org/10.1002/psc.2955>
46. Harris MR, Coote PJ. Combination of caspofungin or anidulafungin with antimicrobial peptides results in potent synergistic killing of *Candida albicans* and *Candida glabrata* in vitro. *Int J Antimicrob Agents*. 2010;35(4):347-356. <https://doi.org/10.1016/j.ijantimicag.2009.11.021>

**How to cite this article:** Lima PG, Souza PFN, Freitas CDT, et al. Anticandidal activity of synthetic peptides: Mechanism of action revealed by scanning electron and fluorescence microscopies and synergism effect with nystatin. *J Pep Sci*. 2020;26:e3249. <https://doi.org/10.1002/psc.3249>